



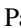




## Clarifying the apparent flattening of the graphene band near the van Hove singularity

Matteo Jugovac <sup>1,2</sup>, Cesare Tresca <sup>3,4</sup>, Iulia Cojocariu,<sup>5</sup> Giovanni Di Santo <sup>2</sup>, Wenjuan Zhao,<sup>2</sup> Luca Petaccia <sup>2</sup>,  
Paolo Moras <sup>1</sup>, Gianni Profeta <sup>3,4</sup> and Federico Bisti <sup>3,\*</sup>

<sup>1</sup>*Istituto di Struttura della Materia-CNR (ISM-CNR), SS 14, Km 163,5, I-34149 Trieste, Italy*

<sup>2</sup>*Elettra Sincrotrone Trieste, Strada Statale 14 km 163.5, I-34149 Trieste, Italy*

<sup>3</sup>*Dipartimento di Scienze Fisiche e Chimiche, Università dell'Aquila, Via Vetoio 10, I-67100 L'Aquila, Italy*

<sup>4</sup>*CNR-SPIN L'Aquila, Via Vetoio 10, I-67100 L'Aquila, Italy*

<sup>5</sup>*Peter Grünberg Institute (PGI-6), Forschungszentrum Jülich GmbH, D-52425 Jülich, Germany*



(Received 5 March 2022; accepted 20 May 2022; published 9 June 2022)

Graphene band renormalization near the van Hove singularity (VHS) has been investigated by angle-resolved photoemission spectroscopy (ARPES) on Li-doped quasifreestanding graphene on a cobalt (0001) surface. The absence of graphene band hybridization with the substrate, the doping contribution well represented by a rigid energy shift, and the excellent electron-electron interaction screening ensured by the metallic substrate offer a privileged point of view for such an investigation. A clear ARPES signal is detected along the *KMK* direction of the graphene Brillouin zone, giving rise to an apparent flattened band. By simulating the graphene spectral function from the density functional theory calculated bands, we demonstrate that the photoemission signal around the *M* point originates from the “tail” of the spectral function of the unoccupied band above the Fermi level. Such an interpretation puts forward the absence of any additional strong correlation effects near the VHS, reconciling the mean-field description of the graphene band structure even in a highly doped scenario.

DOI: [10.1103/PhysRevB.105.L241107](https://doi.org/10.1103/PhysRevB.105.L241107)

The superconducting phase in a twisted graphene bilayer [1] has strongly renewed the interest in flat-band materials, in which a nearly undispersed (flat) energy band is present in a relevant portion of the Brillouin zone. A material presenting a flat band near the Fermi level ( $E_F$ ) is more inclined to manifest exotic electronic phases since any small electronic interactions could be strongly enhanced by the divergent density of states (DOS) coming from this low dispersing band. Therefore, the presence of such DOS singularity is the source for strong electronic instabilities able to open a gap near  $E_F$ , possibly developing a new symmetry breaking ground state. Those instabilities can drive the system to develop magnetic orders [2–9], superconducting states [1,5,10–13], or charge density wave phases [5].

The strategies to get DOS singularity are many, and graphene holds an enormous potential in this field. It emerges from graphene moiré physics at magic angles in connection with a flat band originating from Dirac band hybridization in a bilayer system, as in twisted graphene bilayers [1,13–15] or in epitaxial multilayer graphene [6,9,16–20]. In addition, a DOS singularity is already present in the band structure of graphene at a saddle point in the unoccupied energy region far from the Dirac point (neutrality), known as the van Hove singularity (VHS) [21]. Thus, an efficient alternative route to reach such DOS singularity is to overdope the quasifreestanding monolayer of graphene, bringing  $E_F$  at VHS [22–28]. However, since it was considered too far in energy from the Dirac point to be accessible by chemical doping or gating, much of the attention shifted to twisted systems [29]. Only in

recent years, improvements in graphene growth on appropriate substrates, deposition techniques [30], and band-structure measurements allowed us to “slowly” increase the amount of charge deposited on monolayer graphene, demolishing the belief that the VHS in graphene could not be reached with present technology.

Recent band-structure measurements of doped graphene have detected relevant deviations from a simple rigid shift of neutral graphene or of the first-principles density functional theory (DFT) band structure. Apart from the general consensus on the band renormalization around 170 meV due to the electron-phonon interaction [31], a strong flattening of the band close to  $E_F$  has been interpreted as originating from electron-electron correlations due to the on-site Coulomb interaction  $U$  [22] or spin fluctuations [27]. However, the interpretation of the experimental results is complicated by the graphene’s band hybridization with dopant atoms and/or intercalant atoms deposited on the substrate. A recent example is represented by Yb 4*f*-orbital anticrossing-type hybridization with a graphene  $\pi^*$  band [30], or by the flat-band formation by hybridization in heavily Cs-doped graphene [32]. Unfortunately, the desirable conditions to observe the VHS in (pure) graphene seem mutually exclusive: growth of a nearly freestanding graphene, but with a negligible interaction with the substrate; use of metallic substrates to screen the electron-electron interaction through the substrate; and heavily doping graphene to reach the VHS point, but avoiding hybridization with dopant electronic states to preserve the graphene band structure.

In this Letter, we successfully realized most of the requirements, reporting data on the electronic structure of heavily Li-doped graphene on Co(0001) probed by angle-resolved

\*federico.bisti@univaq.it

photoemission spectroscopy (ARPES) and predicted by first-principles calculations. We observed graphene bands over a large energy range, excellently described by density functional theory with local energy functionals and marginal renormalization of the bandwidth. We demonstrate that the presence of a spectral signal along the  $\Gamma$ - $M$  direction, resembling an apparent strongly renormalized (flattened) band close to  $E_F$ , can be instead clearly reproduced by DFT bands with a careful simulation of the spectral function. Thus the only detectable many-body interaction still holding in graphene (beyond the mean-field DFT) is represented by the electron-phonon coupling, which we observed as a kink in the band dispersion.

Pristine monolayer [epitaxial ( $1 \times 1$ )] graphene samples were prepared *in situ* under ultrahigh vacuum conditions by chemical vapor deposition (CVD) on Co(0001) thin films (about 10 nm) epitaxially grown on W(110), using ethylene as the carbon precursor [33]. To decouple graphene from the Co substrate (making it quasifreestanding), lithium was evaporated (while keeping the sample at 80 K) from commercial SAES metal dispensers and intercalated at room temperature (see Supplemental Material for the graphene growth Li intercalation process [34]). From this doping level, we successfully achieved additional doping, further depositing lithium while keeping the sample temperature at 80 K, thus sandwiching graphene between two lithium monolayers (see below). ARPES data were collected at the BaDEIPh [35] (VUV-Photoemission) beamline of the Elettra synchrotron (Trieste, Italy) using 33 (40) eV photon energy, keeping the sample at 80 (20) K. The total energy and angular resolutions were set to 20 meV (full width at half maximum of the Gaussian model fitting the experimental Fermi edge) and  $0.1^\circ$ , respectively.

We predicted the electronic structure of this heavily doped graphene, modeling it by first-principles DFT (see Supplemental Material for computational details [34]).

The alkali metal atoms were adsorbed (and intercalated) on the hollow site of graphene [36] in a  $\sqrt{3} \times \sqrt{3}$ - $R30^\circ$  reconstruction (see Fig. 1 for a representation of the structural model). The predicted band structure is reported in Fig. 1 (see also Fig. S3 of the Supplemental Material for the system without additional Li on top of graphene [34]). The carbon projected states (blue points) are nearly indistinguishable from the freestanding graphene's band structure (red line), indicating that this structural model realizes a completely decoupled graphene from the substrate. In addition, the magnetic exchange field of the substrate (which is spin polarized) is not affecting the graphene. But, more importantly, the doping level reached is such that the VHS at the  $M$  point should be occupied.

At this point, experimental confirmation is crucial. In Fig. 2, we report the ARPES overview of the Dirac cone for the sample after a first step of Li intercalation (leading only to the graphene/substrate decoupling) and a further deposition step to reach the highest possible doping level (see Supplemental Material for the doping saturation level [34]). The energy position reached by the Dirac point is of  $-1.58$  eV. It is important to note that we are not able to distinguish a gap opening at the Dirac point, thus we exclude any relevant hybridization of the graphene with the Li atoms or with the substrate, meeting the first two requirements listed in the

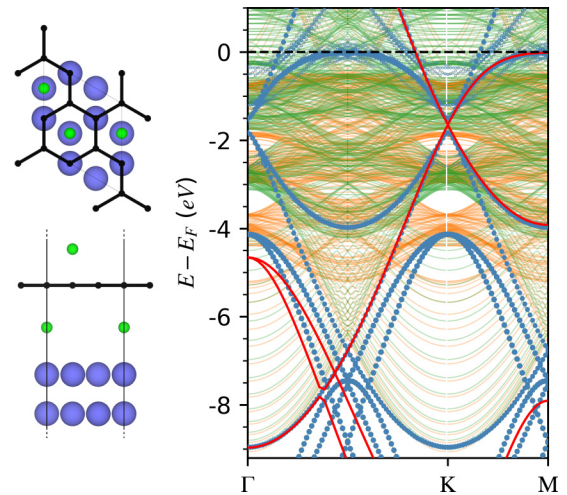


FIG. 1. On the left, the atomic model of Li (green) intercalated graphene (black) supported by the Co substrate (blue). On the right, the spin-up (green) and spin-down (orange) electronic band structures for the overall system. Blue dots represents the carbon  $p_z$ -orbital weight for the states. The red line is the electronic band structure for an isolated graphene layer shifted by  $-1.58$  eV.

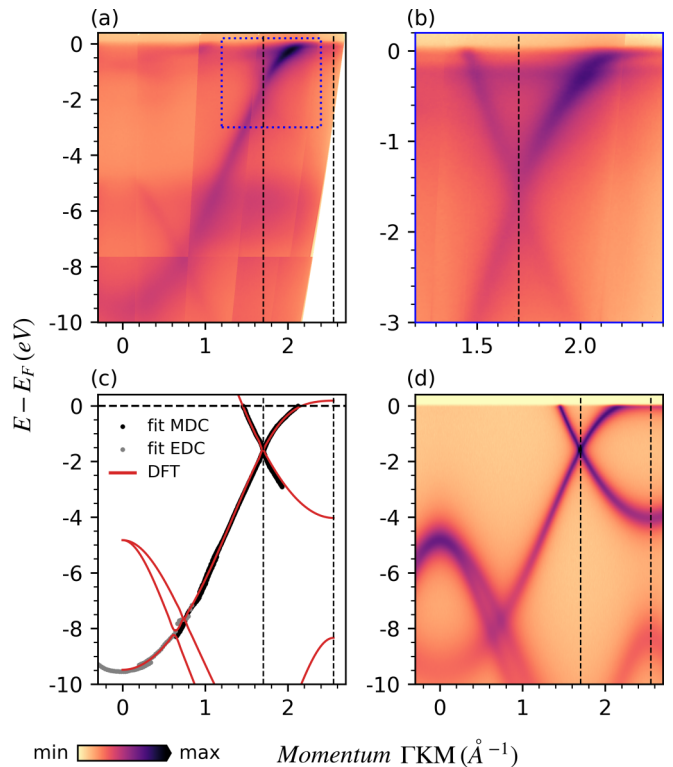


FIG. 2. Graphene Dirac cone dispersion along the  $\Gamma$  $K$  $M$  direction of the Li/Gr/Li/Co system. (a) ARPES spectra using  $p$  polarization. (b) Linear combination of the  $s$ - and  $p$ -polarization ARPES signals near the Dirac point. (c) Extracted band dispersions from the MDC and EDC analysis (black and gray dots, respectively) are reported with stretched (by a factor of 1.08) PBEsol DFT calculations. (d) Simulated spectral function derived from stretched DFT theoretical dispersion. Data in (a), (b), and (d) reported using a square root color scale.

introduction. Lithium is indeed able to detach the graphene layer, as suggested by our theoretical calculation, and in analogy to what was obtained on the same substrate with Si [37] and O [38] intercalation. However, lithium brings further doping. The observed overall doping is quite high, but the actual occupancy of the VHS is not as obvious. Apart from the dominant graphene spectral signal, a small and flat feature is detected at around  $-0.2$  eV, which we attribute to emission from the  $3d$  bands of the cobalt substrate (see Supplemental Material [34]). However, we cannot exclude the possibility of the presence of a flat-band feature observed in other similar systems near the VHS at similar binding energies, which was ascribed to polaron formation due to the coupling with optical phonons [22,27,30] (see Supplemental Material on the possible presence of the polaron band [34]). In order to gain a more quantitative analysis of the graphene  $\pi$ -band dispersion, the momentum (energy) dispersion curves MDCs (EDCs) have been analyzed for the high (low) dispersing part of the  $\pi$  bands. The data are reported in Fig. 2(c), along with the results of the Perdew-Burke-Ernzerhof functional for solids (PBEsol) DFT calculation on isolated graphene. In order to match the experimental data, a marginal renormalization of the theoretical bandwidth is needed by a factor of 1.08, owing to the highly metallic character of the substrate, which guarantees an excellent screening of the Coulomb interaction (which strongly renormalizes graphene bands when grown on insulating substrates [39]). Within this picture, the unoccupied part of the  $\pi^*$  band around the  $M$  point is extremely close to the Fermi level (within 0.18 eV), resulting in a “flat signal” extending along the  $KMK$  direction (visible at the  $E_F$ ), which can thus find a natural origin in the energy broadening stemming from the photoemission final state lifetime. Other additional many-body effects, beyond the mean-field DFT, are not required to explain the graphene band structure. The correlation between the finite electronic final state lifetime value with an unavoidable energy broadening of the probed signal is an explicit manifestation of the particle-wave duality nature of electrons, as described by the Bohr derivation of the uncertainty principle [40]. To demonstrate this effect, in Fig. 2(d) we report the simulated photoemission signal as Lorentzians centered at the DFT eigenvalues ( $E_b$ ), with a Landau’s Fermi-liquid energy-dependent width as  $\gamma = \gamma_0 + \gamma_1 \cdot Eb^2$  with  $\gamma_0 = 0.15$  eV and  $\gamma_1 = 0.01$  eV $^{-1}$ , tuned from the experimental EDC data analysis. The agreement with the experimental curve is indeed very good.

Additional convincing proof comes from the simulation of the Fermi surface as reported in Fig. 3. The MDC analysis of the ARPES signal, reported in Fig. 3(a), is exactly matched by the (renormalized) DFT modes as shown in Fig. 3(b) (the excellent agreement with the theoretical model is also demonstrated in Fig. S5 of the Supplemental Material for different isoenergy maps [34]). The tail extending along the  $KMK$  direction point, reported in Fig. 3(c), is perfectly reproduced by the simulated spectra. To increase even more the simulation fidelity, in Fig. 3(d) we considered also the effect of light polarization in the selection rules. In the isolated graphene case, eigenfunctions are symmetric or antisymmetric with respect to the mirror plane passing between the two carbon atoms of the graphene unit cell. By considering the final state as symmetric with respect to this mirror plane (as in our case, or

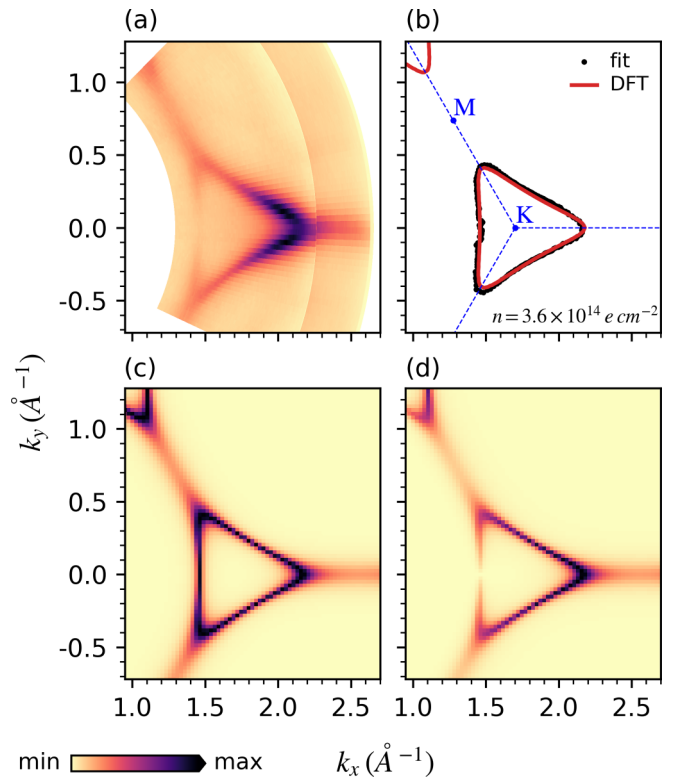


FIG. 3. Fermi surface of the Li/Gr/Li/Co system. (a) ARPES spectra using  $p$  polarization. (b) Extracted band dispersion from MDC analysis (black dots) is reported along with the stretched (by a factor of 1.08) PBEsol DFT calculations (red curve). Simulated spectral function, derived from the stretched DFT theoretical dispersion in (b), without (c) and with (d) the light polarization selection rules. Data reported using a linear color scale.

in general for a pure free-electron final state), then depending on the light polarization symmetry with respect to this plane, we select the photoemission from symmetric or antisymmetric initial states [41]. The simulated spectra are then derived considering this weight in the signal intensity (see Supplemental Material for its exact evaluation [34]). The net result is a vanishing signal in the middle of one side of the Fermi-surface triangle, clearly observed in the experiment [Fig. 3(a)] and perfectly predicted by the simulation in Fig. 3(d) (the same effect is obviously acceptable for the analog isoenergy map below the Dirac point at  $-3.7$  eV, as shown in Fig. S6 of the Supplemental Material [34]). The observed polarization effects are solid confirmation of the absence of any relevant additional interaction on top of graphene since its fundamental mirror plane symmetry is not destroyed (by doping) but perfectly intact, again pointing to the realization of freestanding heavily doped graphene.

From the Fermi-surface area extension we can estimate an effective electron doping of about  $3.6 \times 10^{14}$  e/cm $^2$ , a value comparable with that reported in the recent literature [22,27]. In particular, McChesney *et al.* [22] decorated graphene with calcium above and below the graphene sheet and by depositing additional potassium atoms were able to shift even more down the Dirac point, at least by 0.1 eV. From what is possible to extract from their Fig. 1, the new Fermi energy enhances

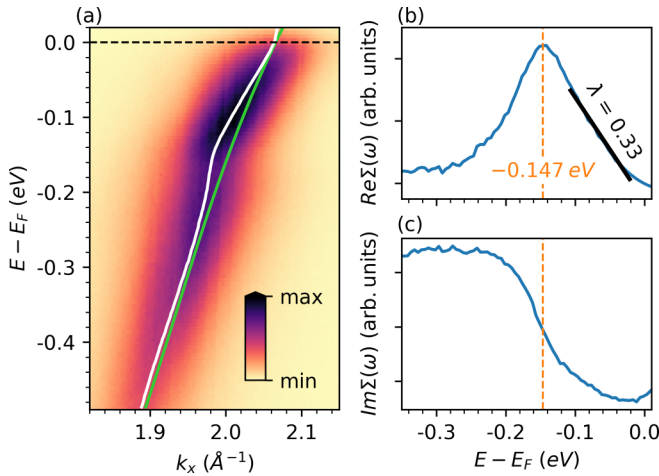


FIG. 4. (a) High-resolution ARPES spectra of graphene band dispersion along the  $\Gamma KM$  direction with the extracted data from MDC analysis (white lines) and the bare bands resulting from the self-consistent analysis (green lines). Data reported using a linear color scale. (b) Self-energy real and (c) imaginary part.

even more the tail effect proposed in our interpretation, but still without reaching (exactly) the VHS.

These findings demonstrate that strong correlation effects due to the electron-electron interaction, invoked to justify the presence of extended van Hove singularities on the Fermi surface of highly doped graphene with alkali metals [22], Gd [27] or Yb [30], could be not necessary to understand the experimental band structure of heavily electron-doped graphene. In addition, such a weak interaction (compared to the fermionic bandwidth) scenario does not preclude the presence of possible nontrivial phases in our system. Indeed, theorized nontrivial phases such as  $d$ -wave superconductivity [10] are based on the assumption of a weak interaction in graphene. Therefore our system, being close to DOS singularity, still holds the promise for hosting such a topological superconductivity phase.

Looking at the experimental ARPES spectra, the more evident deviation from the mean-field band structure is the well-known kink feature at around  $-170$  meV, which represents the only manifestation of many-body effects relevant near the Fermi level even near the VHS. In Fig. 4 we report the kink analysis for the present system, using the same computational analysis as in Ref. [31]. In this case, in order

to reduce the spectral function “tail” signal near the Fermi energy (which can interfere with the fitting procedure), we used a slightly underdoped ( $2.5 \times 10^{14} e/cm^2$ ) system with respect to the data shown before [see Fig. S2(g) of the Supplemental Material and the related discussion [34]], considering that for the purpose of this analysis the overall doping is not so relevant. Interestingly, we notice an unexpected significant energy shift of the kink with respect to the value of the highly doped system with Li ( $-169$  meV) [31], which is now centered at  $-147$  meV, representing the characteristic  $E_{2g}$  phonon frequency. This shift is even larger than that observed in graphene completely substituted with  $^{13}C$  ( $-162$  meV) [31] and cannot be explained by an artificial error due to data manipulation. The observed softening of the phonon modes is a natural consequence of the effect of Li decoration on both sides of graphene and of the increased doping level: Indeed, first-principles theoretical calculations of phonon dispersion for a graphene layer decorated on both sides have correctly predicted this softening (see Supplemental Material of Ref. [36]). This represents additional, indirect confirmation of the physical realization of a heavily doped ideal freestanding graphene.

In conclusion, Li decoupled and highly doped graphene on Co(0001) resulted in an excellent realization of an ideal freestanding graphene layer in a highly doped regime, without spurious effects such as substrate or dopant interactions. From the analysis of its band structure, we were able to demonstrate, at the same time, that (i) a single electron picture is capable of explaining the ARPES signal only including a relatively small energy renormalization, but without invoking strong correlation effects to induce band-structure flattening near the VHS, (ii) ARPES spectra can show a signal from the unoccupied band if it sufficiently close to the Fermi level within the thermal broadening of the Fermi distribution and the lifetime of the photoemission hole, (iii) the only detectable many-body feature, beyond the mean-field DFT, near the Fermi level is the electron-phonon kink, and (iv) the present system shows a phonon softening induced by the alkali metal decoration on both sides of graphene.

The authors acknowledge Elettra Sincrotrone Trieste for providing access to its synchrotron radiation facilities. G.P. wishes to acknowledge financial support from the Italian Ministry for Research and Education through PRIN-2017 project “Tuning and understanding Quantum phases in 2D materials - Quantum 2D” (IT-MIUR Grant No. 2017Z8TS5B).

[1] Y. Cao, V. Fatemi, S. Fang, K. Watanabe, T. Taniguchi, E. Kaxiras, and P. Jarillo-Herrero, Unconventional superconductivity in magic-angle graphene superlattices, *Nature (London)* **556**, 43 (2018).  
 [2] A. Mielke, Ferromagnetic ground states for the Hubbard model on line graphs, *J. Phys. A: Math. Gen.* **24**, L73 (1991).  
 [3] H. Tasaki, Ferromagnetism in the Hubbard Models with Degenerate Single-Electron Ground States, *Phys. Rev. Lett.* **69**, 1608 (1992).

[4] A. Mielke and H. Tasaki, Ferromagnetism in the Hubbard model, *Commun. Math. Phys.* **158**, 341 (1993).  
 [5] C. Honerkamp, Density Waves and Cooper Pairing on the Honeycomb Lattice, *Phys. Rev. Lett.* **100**, 146404 (2008).  
 [6] B. Pamuk, J. Baima, F. Mauri, and M. Calandra, Magnetic gap opening in rhombohedral-stacked multilayer graphene from first principles, *Phys. Rev. B* **95**, 075422 (2017).  
 [7] M. Calandra, Phonon-Assisted Magnetic Mott-Insulating State in the Charge Density Wave Phase of Single-Layer  $1T$ -NbSe<sub>2</sub>, *Phys. Rev. Lett.* **121**, 026401 (2018).

- [8] C. Tresca and M. Calandra, Charge density wave and spin 1/2 insulating state in single layer 1T-NbS<sub>2</sub>, *2D Mater.* **6**, 035041 (2019).
- [9] M. Campetella, J. Baima, N. M. Nguyen, L. Maschio, F. Mauri, and M. Calandra, Hybrid-functional electronic structure of multilayer graphene, *Phys. Rev. B* **101**, 165437 (2020).
- [10] R. Nandkishore, L. S. Levitov, and A. V. Chubukov, Chiral superconductivity from repulsive interactions in doped graphene, *Nat. Phys.* **8**, 158 (2012).
- [11] E. H. da Silva Neto, P. Aynajian, A. Frano, R. Comin, E. Schierle, E. Weschke, A. Gyenis, J. Wen, J. Schneeloch, Z. Xu, S. Ono, G. Gu, M. Le Tacon, and A. Yazdani, Ubiquitous interplay between charge ordering and high-temperature superconductivity in cuprates, *Science* **343**, 393 (2014).
- [12] R. Comin, A. Frano, M. M. Yee, Y. Yoshida, H. Eisaki, E. Schierle, E. Weschke, R. Sutarto, F. He, A. Soumyanarayanan, Y. He, M. Le Tacon, I. S. Elfimov, J. E. Hoffman, G. A. Sawatzky, B. Keimer, and A. Damascelli, Charge order driven by Fermi-arc instability in Bi<sub>2</sub>Sr<sub>2-x</sub>La<sub>x</sub>CuO<sub>6+δ</sub>, *Science* **343**, 390 (2014).
- [13] X. Lu, P. Stepanov, W. Yang, M. Xie, M. A. Aamir, I. Das, C. Urgell, K. Watanabe, T. Taniguchi, G. Zhang, A. Bachtold, A. H. MacDonald, and D. K. Efetov, Superconductors, orbital magnets and correlated states in magic-angle bilayer graphene, *Nature (London)* **574**, 653 (2019).
- [14] A. Kerelsky, L. J. McGilly, D. M. Kennes, L. Xian, M. Yankowitz, S. Chen, K. Watanabe, T. Taniguchi, J. Hone, C. Dean, A. Rubio, and A. N. Pasupathy, Maximized electron interactions at the magic angle in twisted bilayer graphene, *Nature (London)* **572**, 95 (2019).
- [15] S. Lisi, X. Lu, T. Benschop, T. A. de Jong, P. Stepanov, J. R. Duran, F. Margot, I. Cucchi, E. Cappelli, A. Hunter, A. Tamai, V. Kandyba, A. Giampietri, A. Barinov, J. Jobst, V. Stalman, M. Leeuwenhoek, K. Watanabe, T. Taniguchi, L. Rademaker, S. J. van der Molen, M. P. Allan, D. K. Efetov, and F. Baumberger, Observation of flat bands in twisted bilayer graphene, *Nat. Phys.* **17**, 189 (2021).
- [16] D. Pierucci, H. Sediri, M. Hajlaoui, J.-C. Girard, T. Brumme, M. Calandra, E. Velez-Fort, G. Patriarche, M. G. Silly, G. Ferro, V. Soulière, M. Marangolo, F. Sirotti, F. Mauri, and A. Ouerghi, Evidence for flat bands near the Fermi level in epitaxial rhombohedral multilayer graphene, *ACS Nano* **9**, 5432 (2015).
- [17] H. Henck, J. Avila, Z. Ben Aziza, D. Pierucci, J. Baima, B. Pamuk, J. Chaste, D. Utt, M. Bartos, K. Nogajewski, B. A. Piot, M. Orlita, M. Potemski, M. Calandra, M. C. Asensio, F. Mauri, C. Faugeras, and A. Ouerghi, Flat electronic bands in long sequences of rhombohedral-stacked graphene, *Phys. Rev. B* **97**, 245421 (2018).
- [18] Y. Henni, H. P. Ojeda Collado, K. Nogajewski, M. R. Molas, G. Usaj, C. A. Balseiro, M. Orlita, M. Potemski, and C. Faugeras, Rhombohedral multilayer graphene: A magneto-Raman scattering study, *Nano Lett.* **16**, 3710 (2016).
- [19] D. Marchenko, D. V. Evtushinsky, E. Golias, A. Varykhalov, T. Seyller, and O. Rader, Extremely flat band in bilayer graphene, *Sci. Adv.* **4**, eaau0059 (2018).
- [20] J. Baima, F. Mauri, and M. Calandra, Field-effect-driven half-metallic multilayer graphene, *Phys. Rev. B* **98**, 075418 (2018).
- [21] A. H. Castro Neto, F. Guinea, N. M. R. Peres, K. S. Novoselov, and A. K. Geim, The electronic properties of graphene, *Rev. Mod. Phys.* **81**, 109 (2009).
- [22] J. L. McChesney, A. Bostwick, T. Ohta, T. Seyller, K. Horn, J. González, and E. Rotenberg, Extended van Hove Singularity and Superconducting Instability in Doped Graphene, *Phys. Rev. Lett.* **104**, 136803 (2010).
- [23] F. Bisti, G. Profeta, H. Vita, M. Donarelli, F. Perrozzi, P. M. Sheverdyeva, P. Moras, K. Horn, and L. Ottaviano, Electronic and geometric structure of graphene/SiC(0001) decoupled by lithium intercalation, *Phys. Rev. B* **91**, 245411 (2015).
- [24] A. Khademi, E. Sajadi, P. Dosanjh, D. A. Bonn, J. A. Folk, A. Stöhr, U. Starke, and S. Forti, Alkali doping of graphene: The crucial role of high-temperature annealing, *Phys. Rev. B* **94**, 201405(R) (2016).
- [25] N. I. Verbitskiy, A. V. Fedorov, C. Tresca, G. Profeta, L. Petaccia, B. V. Senkovskiy, D. Y. Usachov, D. V. Vyalikh, L. V. Yashina, A. A. Eliseev, T. Pichler, and A. Grüneis, Environmental control of electron-phonon coupling in barium doped graphene, *2D Mater.* **3**, 045003 (2016).
- [26] C. Tresca, N. I. Verbitskiy, A. Grüneis, and G. Profeta, Ab initio study of the (2 × 2) phase of barium on graphene, *Eur. Phys. J. B* **91**, 165 (2018).
- [27] S. Link, S. Forti, A. Stöhr, K. Küster, M. Rösner, D. Hirschmeier, C. Chen, J. Avila, M. C. Asensio, A. A. Zakharov, T. O. Wehling, A. I. Lichtenstein, M. I. Katsnelson, and U. Starke, Introducing strong correlation effects into graphene by gadolinium intercalation, *Phys. Rev. B* **100**, 121407(R) (2019).
- [28] I. Antoniazzi, T. Chagas, M. J. Matos, L. A. Marçal, E. A. Soares, M. S. Mazzoni, R. H. Miwa, J. M. J. Lopes, Â. Malachias, R. Magalhães-Paniago, and M. H. Oliveira Jr., Oxygen intercalated graphene on SiC(0001): Multiphase SiO<sub>x</sub> layer formation and its influence on graphene electronic properties, *Carbon* **167**, 746 (2020).
- [29] G. Li, A. Luican, J. M. B. Lopes dos Santos, A. H. Castro Neto, A. Reina, J. Kong, and E. Y. Andrei, Observation of Van Hove singularities in twisted graphene layers, *Nat. Phys.* **6**, 109 (2010).
- [30] P. Rosenzweig, H. Karakachian, D. Marchenko, K. Küster, and U. Starke, Overdoping Graphene Beyond the van Hove Singularity, *Phys. Rev. Lett.* **125**, 176403 (2020).
- [31] F. Bisti, F. Priante, A. V. Fedorov, M. Donarelli, M. Fantasia, L. Petaccia, O. Frank, M. Kalbac, G. Profeta, A. Grüneis, and L. Ottaviano, Electron-phonon coupling origin of the graphene π\*-band kink via isotope effect, *Phys. Rev. B* **103**, 035119 (2021).
- [32] N. Ehlen, M. Hell, G. Marini, E. H. Hasdeo, R. Saito, Y. Falke, M. O. Goerbig, G. Di Santo, L. Petaccia, G. Profeta, and A. Grüneis, Origin of the flat band in heavily Cs-doped graphene, *ACS Nano* **14**, 1055 (2020).
- [33] M. Jugovac, F. Genuzio, E. L. Gonzalez, N. Stojić, G. Zamborlini, V. Feyer, T. O. Menteş, A. Locatelli, and C. M. Schneider, Role of carbon dissolution and recondensation in graphene epitaxial alignment on cobalt, *Carbon* **152**, 489 (2019).
- [34] See Supplemental Material at <http://link.aps.org/supplemental/10.1103/PhysRevB.105.L241107> for computational details, graphene growth and Li intercalation process, doping saturation level, possible presence of a polaron band, iso-energy maps around the Dirac point, and weighted simulated signal.
- [35] L. Petaccia, P. Vilmercati, S. Gorovikov, M. Barnaba, A. Bianco, D. Cocco, C. Masciovecchio, and A. Goldoni, BaD

- ElPh: A 4m normal-incidence monochromator beamline at Elettra, *Nucl. Instrum. Methods Phys. Res., Sect. A* **606**, 780 (2009).
- [36] G. Profeta, M. Calandra, and F. Mauri, Phonon-mediated superconductivity in graphene by lithium deposition, *Nat. Phys.* **8**, 131 (2012).
- [37] D. Y. Usachov, A. V. Fedorov, O. Y. Vilkov, I. I. Ogorodnikov, M. V. Kuznetsov, A. Grüneis, C. Laubschat, and D. V. Vyalikh, Electron-phonon coupling in graphene placed between magnetic Li and Si layers on cobalt, *Phys. Rev. B* **97**, 085132 (2018).
- [38] M. Jugovac, F. Genuzio, T. O. Menteş, A. Locatelli, G. Zamborlini, V. Feyer, and C. M. Schneider, Tunable coupling by means of oxygen intercalation and removal at the strongly interacting graphene/cobalt interface, *Carbon* **163**, 341 (2020).
- [39] C. Hwang, D. A. Siegel, S.-k. Mo, W. Regan, A. Ismach, Y. Zhang, A. Zettl, and A. Lanzara, Fermi velocity engineering in graphene by substrate modification, *Sci. Rep.* **2**, 590 (2012).
- [40] N. Bohr, The quantum postulate and the recent development of atomic theory, *Nature (London)* **121**, 580 (1928).
- [41] F. Bisti, V. A. Rogalev, M. Karolak, S. Paul, A. Gupta, T. Schmitt, G. Güntherodt, V. Eyert, G. Sangiovanni, G. Profeta, and V. N. Strocov, Weakly-Correlated Nature of Ferromagnetism in Nonsymmorphic CrO<sub>2</sub> Revealed by Bulk-Sensitive Soft-X-Ray ARPES, *Phys. Rev. X* **7**, 041067 (2017).